Properties of Electrodeposited Cadmium Sulfide Films for Photovoltaic Devices With Comparison to CdS Films Prepared by Other Methods

Figen KADIRGAN[*]
Department of Chemistry, Istanbul Technical University,
80626, Maslak, İstanbul-TURKEY
Duli MAO, Wenjie SONG, Tim OHNO
Department of Physics, Colorado School of Mines,
Golden, 80401, Colorado-USA
Brian McCANDLESS
Institute of Energy Conversion, Delaware University,
Newark, DE 19716-USA

Films of CdS for photovoltaic devices were electrochemically deposited on tin oxide coated glass substrates at different conditions. The films were found to be smooth and uniform with a small grain size. X-ray diffraction measurement and analysis indicated a hexagonal phase rather than the cubic phase. The surface composition of the films was investigated by Auger Spectroscopy. Electrochemical deposition parameters were studied to obtain the optimum conditions for the best CdS films. Our films are compared from the pinhole number and particulate point of view with the films prepared by other methods.

Key words: Electrodeposition of CdS, CdS/CdTe solar cells, photovoltaic devices

Introduction

Polycrystalline thin film solar cells based on n CdS/p CdTe are good candidates[1-7] from the viewpoint of simplicity, scalability and economic fabrication. Electrochemical deposition techniques for this cell have attracted considerable attention[3-5].

Technologically, the electrochemical deposition method through the influence of potential, temperature, pH and composition of reactants offers excellent control over the properties of semiconductor films. In these solar cells, the n-CdS thin film constitutes the most significant component. The CdS film allows transportation of majority carriers for collection at the negative electrode. Hence, the CdS film stoichiometry, crystalline structure, grain morphology and electrical properties are extremely important for fabrication of efficient cells. CdTe films are deposited over the CdS films forming the p-n junction. The cell structure is

---

[*] Corresponding author

such that the photoabsorbing carrier generating CdTe films are electrodeposited over performed CdS films. Thus the above mentioned properties of the CdS films exert significant influence over the growth behaviour of subsequently formed active layers and may even modify their characteristics to detriment to solar cell performance. A detailed knowledge of the microstructure of CdS thin films with regard to deposition controlling parameters is thus essential.

It is observed that the growth of CdS during electrodeposition from diethylene glycol solution at a CdS surface is controlled by the reduction of sulfur[8]. The reduction of sulfur in an aprotic solvent (DMSO) is found to be a two-stage process[9].

The formation of CdS thin film by cathodic deposition of Cd^{2+} ions from a solution containing sulphur on different substrates (Pt, Mo, Al) is described. Also these authors have studied the influence of the substrate on the formation and morphology Fatas et al. [10]. Power et al. [11] and Das et al. [12] investigated the cathodic formation of CdS films from thiosulfate solutions. McCandless et al. [13] investigated the galvanic deposition of CdS. They found that the CdS deposition rate was controlled by the reduction rate of Cd, which for galvanic deposition was determined primarily by Cd ion concentration and to a lesser degree by temperature and agitation. Similar properties to evaporated CdS films were also found.

In this paper, we fabricated CdS thin films by electrodeposition over tin oxide (TO) and indium tin oxide (ITO) coated glass electrodes. We have investigated electrolyte composition, pH and temperature effects on the deposition time, microstructure, crystalline orientation and surface composition of CdS films. We have chosen deposition time as comparison criteria to able to observe if the electrochemical deposition is really competitive with other preparation methods from the viewpoint of commercial application. We also compared the surface properties of electrodeposited CdS films with the films grown by other methods.
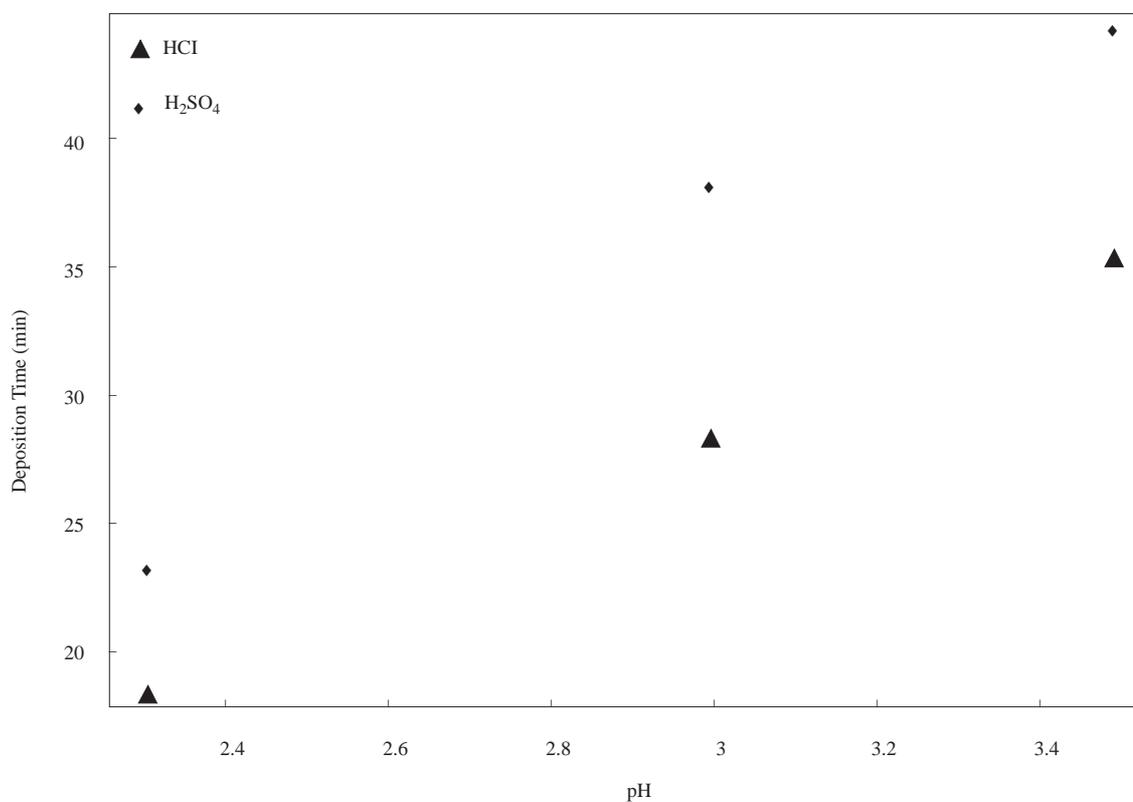
Figure 1. Deposition time-pH curves for the CdS films prepared in 0.2M Cd^2, 0.05 M $S_2O_3^{2-}$, 90°C, 0.17 C/cm^2 using either HCl or H_2SO_4 as the acid ▲ HCl ♦ H_2SO_4

Experimental

Electrodeposited CdS films were prepared in a classical double wall, three electrode cell under nitrogen using a 0.2M $CdCl_2$ solution on SnO_2 coated glassses as the substrates. Solutions were prepared using water purified by a Millipore-Mili-Q filtration system. TO or ITO coated glasses were cleaned with a special detergent in an ultrasonic bath and rinsed and then ultrasonically cleaned with water. As the reference and counter electrodes saturated calomel and glassy glass electrodes were used respectively. The pH was changed from 2 up to 4 by using either HCI or H_2SO_4. The $Na_2S_2O_3$ concentration was varied between 0.01M and 0.05M. All chemicals were Aldrich analytical grade. Deposition was performed applying a potential of -0.6V/SCE at $80°C$ and $90°C$. The morphology and structural properties of these films were analysed by using scanning electron microscopy (SEM) and X-ray diffraction (XRD). Surface composition of the films was determined by scanning Auger spectroscopy. Microscopic examination was performed to determine the pinhole and embedded particulates. Before examination, the pieces were ultrasonically rinsed in methanol and dried under pressurized argon. For the Institute of Energy Conversion (IEC) samples, the CdS films were on corning 7059 glass/ITO, with ITO sputtered at IEC. The University of Toledo samples were on different substrates and sputtering conditions.

Results and Discussion

Film forming process for CdS

The resulting electrodeposited CdS thin films appear uniform and smooth in terms of film quality. The reaction mechanism of CdS formation involves 2 electron transfer and it follows the reaction (10-12):
$Cd^{2+} + S_2O_3^{2-} + 2e^- \rightarrow CdS + SO_3^{2-}$
Electrodeposition reaction of CdS is dependent of pH, because of a disproportion reaction of the thiosulphate ions, which may occur depending on the pH values of the electrolyte as follows:
$S_2O_3^{2-} \rightarrow S + SO_3^{2-}$
Lowering the pH to 2 causes the decomposition of $S_2O_3^{2-}$ and forms colloidal sulphur.
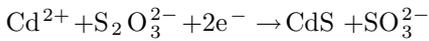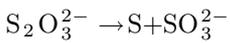
Effect of electrolyte nature and pH on the film formation process:

The pH was adjusted from 2 to 4 using either HCI or H_2SO_4. During the electrodeposition of CdS film, film thickness control determines also the degree of control possible over the stochiometry and the morphology of the film obtained. The total charge passed through the plating circuit deposition gives a good measure of the amount of materials deposited. Once the average thicknesses of corresponding film are experimentally determined (by α-step, Tencor), the variables playing a role on plating efficiency may be observed by controlling the plating time at constant potential. After the determination of efficiency, the average thickness of the films can be controlled in-situ by the plating time. Hence, electrochemical deposition time has been chosen as comparison criteria to able to observe whether the electrochemical deposition is really competitive with the other preparation methods from the commercial application viewpoint. Deposition time is defined as the time for reaching a constant charge per unit area (0.17 $C.cm^{-2}$) in different pH values. Fig.1 shows the deposition time as a function of pH. It is observed that the deposition time of CdS film formation changes depending on the acid and the pH. Deposition time was longer in the H_2SO_4 containing electrolyte. It increases at higher pH values.

Variation of Faradaic Efficiency as a function of pH:

The faradaic efficiency (a number between 0-1) can be calculated by the following equation:

Faradaic efficiency = Charge involved in the film formation, Q', (determined from thickness measurements)/Total charge passed during the deposition, Q

$Q = t \times 6442,2$

where Q' is charge per unit area (coulomb.cm^{-2}) and t is thickness (cm). Plating efficiency was calculated in 0.2M Cd^{2+} +0.05M S$_2$O$_3^{2-}$ solution at 90$°$C as a function of pH. Either HCI or H$_2$SO$_4$ was used to adjust the pH. (fig.2) It was observed that increasing the pH increases the plating efficiency. 53% efficiency was calculated for pH=3. The low value of efficiency may be explained either by H$_2$ evolution at low pH values or by ohmic drop with the formation of CdS film on the electrode surface which is less conductive. It is also observed that plating efficiency is higher in the same pH values using the H$_2$SO$_4$ as the electrolyte. This may be explained by etching effect of HCI on the CdS film surface.
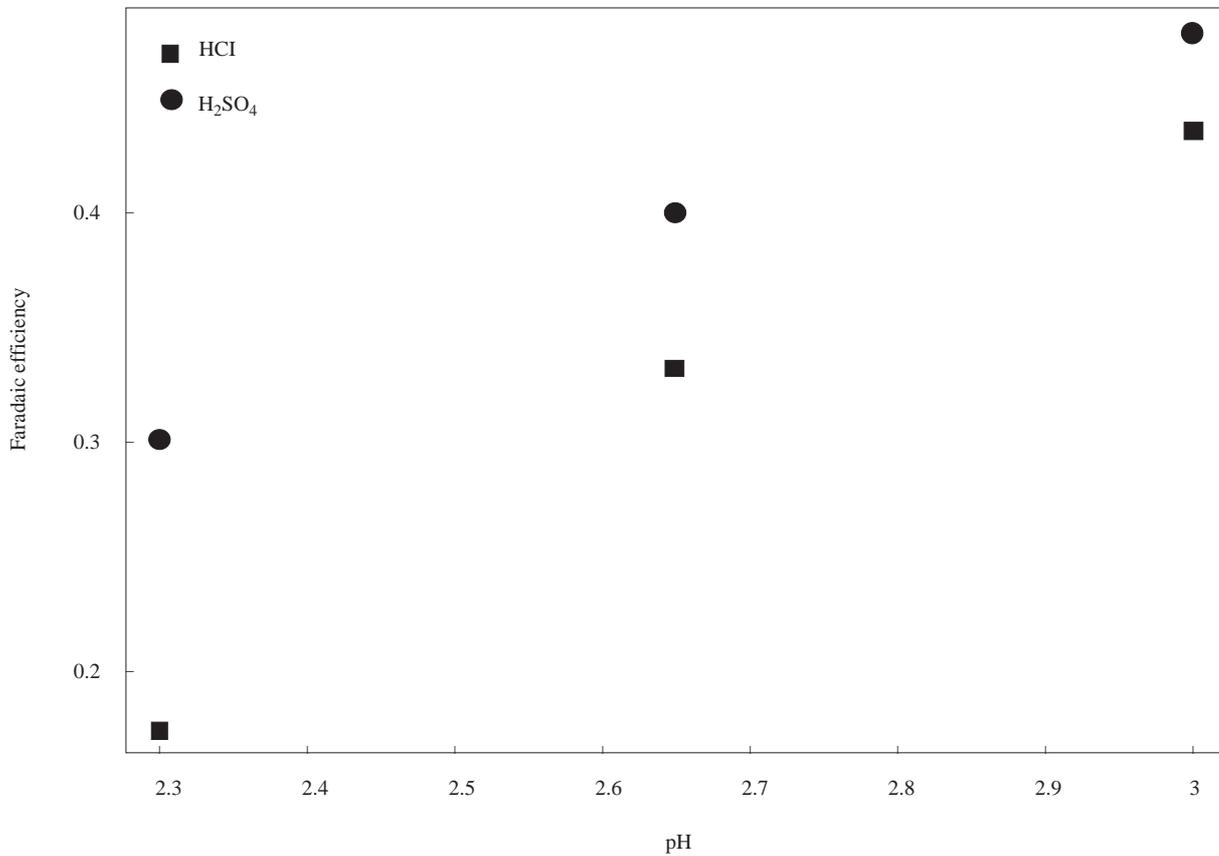
Figure 2. Faradaic efficiency as a function of pH (0.2M Cd^{2+} (0.05M S$_2$O$_3^{2-}$ solution at 90$°$C) adjusting HCI ■HCI ● H$_2$SO$_4$

Variation of charge as a function of thickness of the CdS film:

The relationship between the CdS film thickness and charge at pH 3 and 90$°$C using 0.2M Cd^{2}+0.05M S$_2$O$_3^{2-}$ + HCI is shown in Fig. 3. The growth rate increases linearly up to 2500 $°$A and reaches to stability. This may explain the etching effect of HCI on the surface at longer deposition times.

24
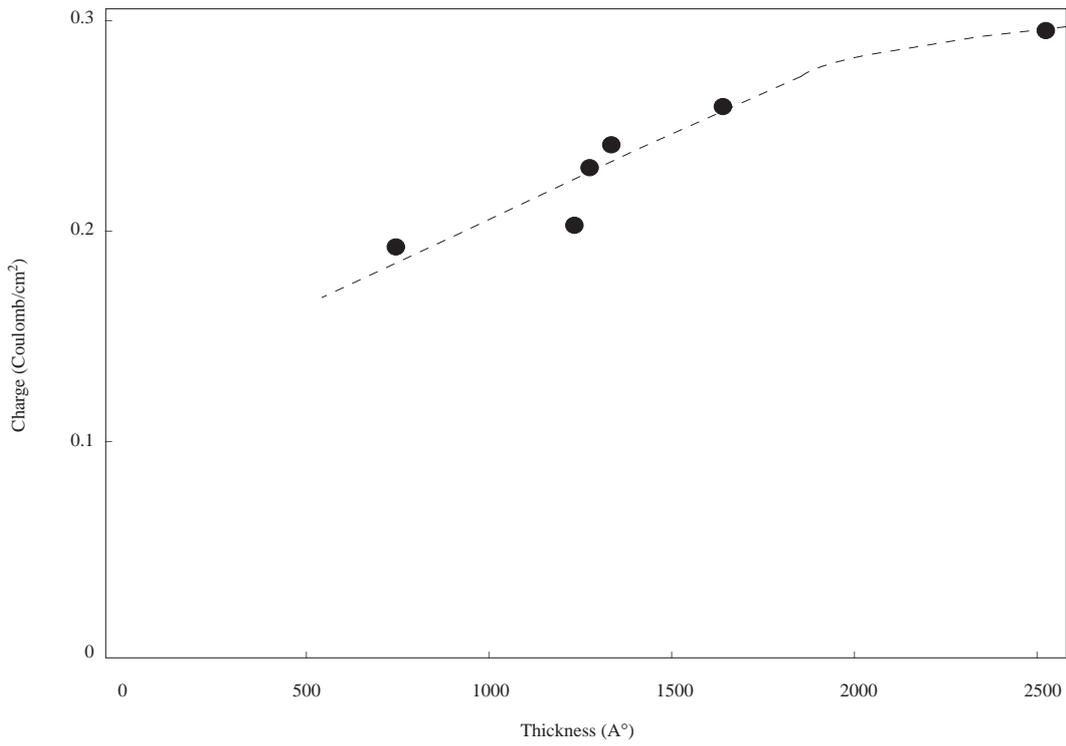
Figure 3. Charge-thickness curve for the CdS films prepared in 0.2M Cd^2 +0.05M $S_2O_3^{2-}$, solution at 90°C and pH 3 adjusting HCI
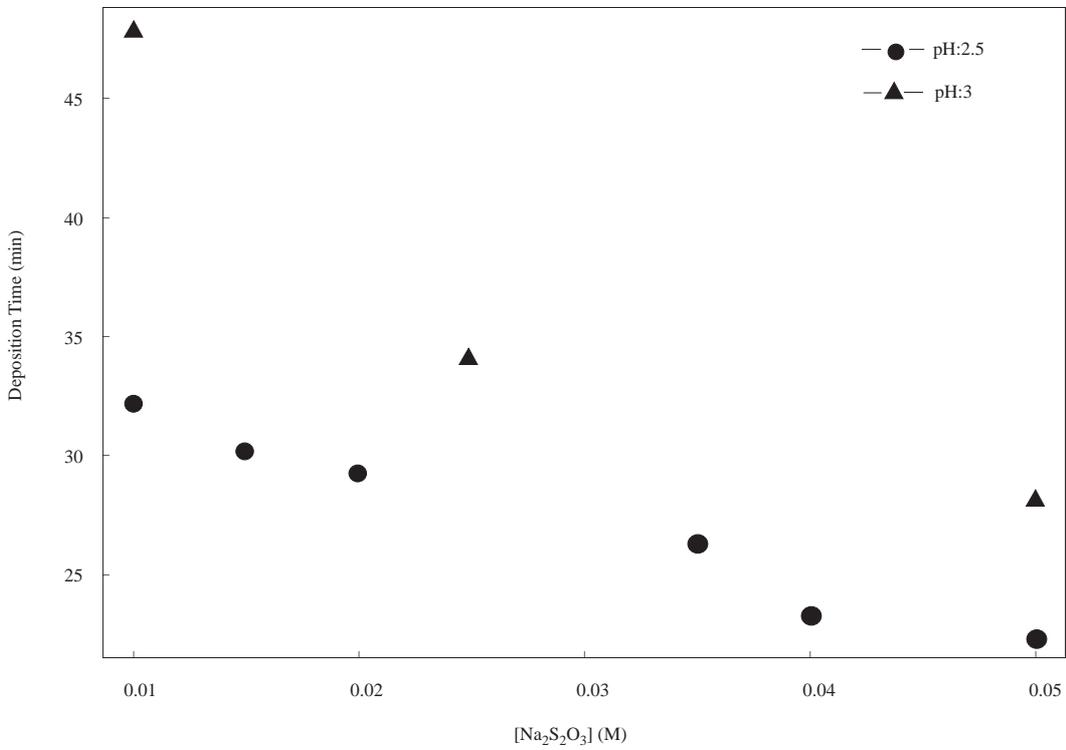
Figure 4. Deposition time as a function of $Na_2S_2O_3$ concentration at two different pH using HCI (0.2M Cd^2, 90°C, Q=0.17.cm^{-2}) ● pH=2.5 ▲ pH=3
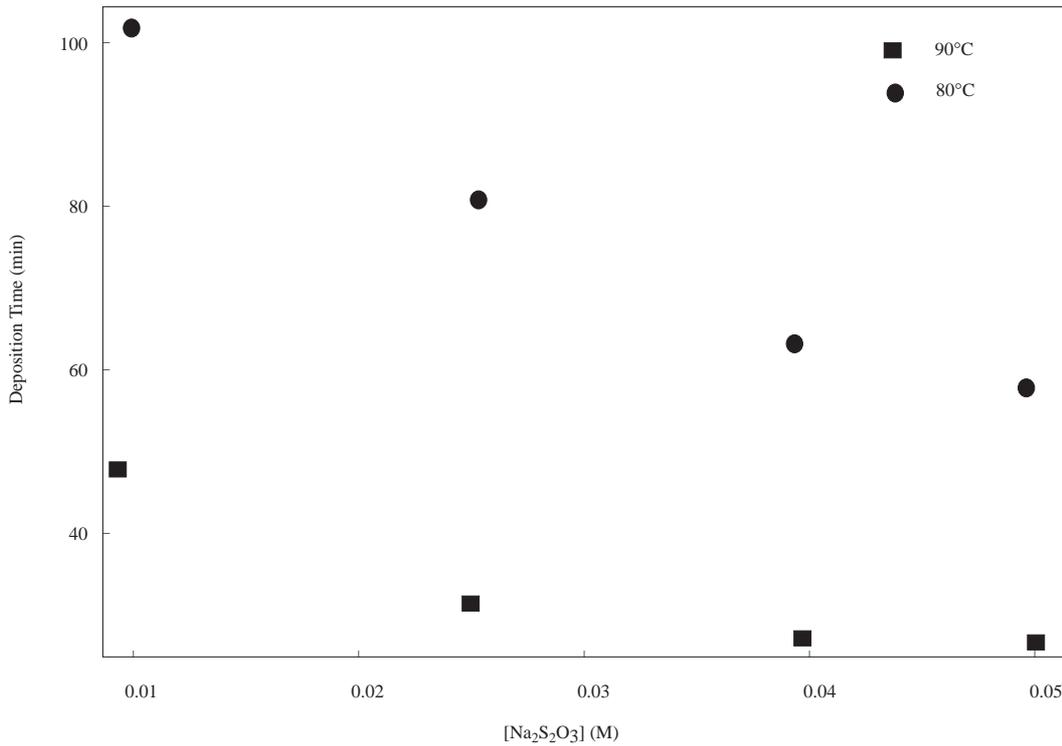
Figure 5. Deposition time as a function of $Na_2S_2O_3$ concentration at two different temperatures using HCI (Cd^2, $Q=0.17.cm^{-2}$, pH=3) ■ t=90°C ● T=80°C

Effect of $S_2O_3^{2-}$ concentration on the plating time:

a) At different pH values: The effect of $Na_2S_2O_3$ concentration on the deposition time at different pH is shown in Fig. 4. The variation of deposition time is sharper at higher pH values. It may be due to either disproportionation reaction of $S_2O_3^{2-}$ ions or the lower efficiency in in lower pH values. Deposition time decreases with increasing $S_2O_3^{2-}$ concentration.

b) At different temperatures: The variation of deposition time is investigated at constant pH (pH=3). It is seen that increasing the temperature and $S_2O_3^{2-}$, deposition time decreases up to 30 minutes (Q=0.17 $C.cm^{-2}$)(Fig.5).

Optical Properties:

The optical transmittance of the CdS films prepared at pH=3, 90°C and pH=2.6, 80°C were measured. Fig. 6 shows the results obtained. The variation of T/(1-R) in the spectral range of 550-900 nm. matches qualitatively those for the samples prepared at two different pH values.
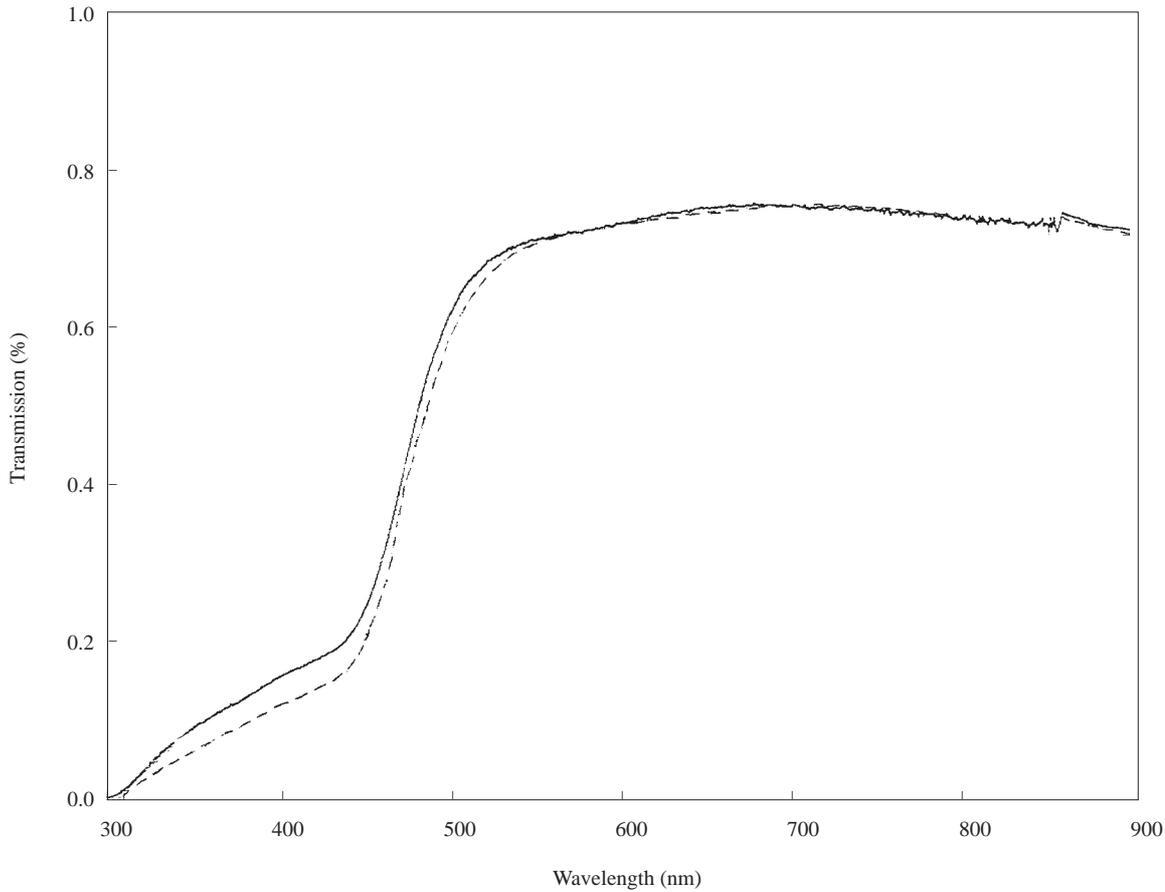
Figure 6. Transmission T/(1-R)/Wavelength curve at two different pH

Microscopic examination was performed to determine the pinhole and embedded particulates. Before examination, the pieces were ultrasonically rinsed in methanol and dried under pressurized argon. Pinholes and the number of surface particulates are calculated for two samples of identical thickness prepared at different conditions. The sample prepared at pH=2.6 has an order of magnitude greater density of pinhole area than the sample prepared at pH=3. First one has over 30 pinholes, while the second has only 9 (Table 1)

Column definitions are as follows: d(CdS)= Thickness, Area h=area of pinholes in survey region, F_h=fractional area of pinholes, Area p=area of particulates in survey region, F_p=fractional area of particulates, F_h+F_p=sum of pinhole and particulate fractional areas.

Table 1 descriptively summarises of pinhole and particulate fractional areas of CdS films prepared by different methods in different universities or research institutes. The University of Toledo and National renewable Laboratory (NREL) samples were grown on different substrates by rf-sputtering [14] and chemical bath deposition (CBD) [15] methods respectively. The CdS films were prepared by physical vapor deposition (PVD) on indium-tin oxide (ITO) sputtered corning 7059 glass in the Institute of Energy Conversion (IEC) [16].

Particulates are included in the survey since they could lead so shunt paths as pinholes in CdS (formed via reaction during treatments) or spikes through the CdTe layer. Their vertical dimension (normal to film plane) was measured as 5-10μm on CBD and sputtered films and $<5\mu$m on PVD films. For the IEC samples made by PVD, the 250°A case exhibited low optical contrast, making pinhole assessment difficult.

Nevertheless, for the other samples the pinhole area increased with decreasing CdS thickness. For the NREL CBD samples, the pinhole area was low but the particulate density was high. EDS examination of the particulates revealed the presence of Sn, Al, Si, and Cl. More specific analysis is needed to determine if these could be attributed to the TCO or the CBD bath. For electrochemically prepared (ED) films (CSM samples), the number of particulates was very low ($\sim$1 per sample). The entire surface was surveyed (in 1 mm. from the edges to discount edges, cutting and tweezer effects are neglected). The sample prepared at pH=2.6 and 80°C had an order of magnitude greater density of pinhole area than sample deposited at pH=3, 90°C.

Table 1. Comparison of CdS films prepared by different methods.

Group	Substrate	Ref.	CdS	d	Area	F_h	Area	F_p	$F_p + F_h$
			Method	(CdS)	h		p		
				(A$^\circ$)	(cm^2)		(cm^2)		
UTol	7059 no O2		Sputter	3000	8E-05	8E-05	2E-04	2E-04	2E-04
UTol	7059 no O2		Sputter	900	4E-06	4E-06	2E-04	2E-04	2E-04
UTol	LOF no O2	[14]	Sputter	500	2E-05	2E-05	2E-04	2E-04	2E-04
UTol	LOF + O2		Sputter	500	0E-00	0	2E-04	2E-04	2E-04
UTol	LOF + O2		Sputter	500	2E-05	2E-05	1E-04	1E-04	1E-04
NREL	SnO2/7059		CBD	1060	1E-05	1E-05	5E-05	4E-05	5E-05
NREL	SnO2/7059	—15]	CBD	400	1E-05	1E-05	6E-05	6E-05	7E-05
CSM	SnO2/7059		ED	1200	5E-05	3E-05	2E-05	1E-05	3E-05
CSM	SnO2/7059		ED	1200	2E-05	5E-06	2E-06	6E-07	6E-06
IEC	ITO/7059		PVD	2000	5E-06	5E-06	4E-06	4E-06	9E-06
IEC	ITO/7059		PVD	1200	2E-05	2E-05	7E-06	7E-06	2E-05
IEC	ITO/7059	[16]	PVD	1000	2E-05	2E-05	4E-06	4E-06	2E-05
IEC	ITO/7059		PVD	700	5E-05	5E-05	4E-06	4E-06	4E-05
IEC	ITO/7059		PVD	250	N/A	N/A	4E-06	4E-06	4E-06

Structural Properties

There are several reports [17−21] on the structural properties of CdS films prepared by chemical bath deposition. However, there is no detailed work on the CdS films prepared by electrodeposition. It is known that high quality as-deposited CdS films have only one preferred orientation corresponding to either cubic (111) or hexagonal (002). But, it is difficult to distinguish these two phases based on the XRD peak position [17,18]. Kaur et al. [22] concluded that the "ion-by-ion" process results in compact films which have pure hexagonal or a mixture of hexagonal and cubic phase. However, cluster-by-cluster process gives rise to porous layers with pure cubic phase. Demir and al. observed that hexagonal CdS has grown on both the (111) [23] and (100) low index planes of Au during the electrochemical growth [24].

Since the XRD peak positions of CdS and TO overlap when the film was prepared on TO substrate, ITO has been chosen as substrate to investigate the structure of CdS. Fig. 7 a and b show the XRD patterns for a ITO/glass alone and CdS film obtained on ITO/glass substrate at pH=3 respectively. The positions of

several peaks were used to determine the CdS phases shown in Table 2; peak positions are closer to those of hexagonal phase than the cubic phase. We have to mention that it is difficult to separate cubic (111) peaks from hexagonal (002) peaks, because they are overlapping in the same regions.
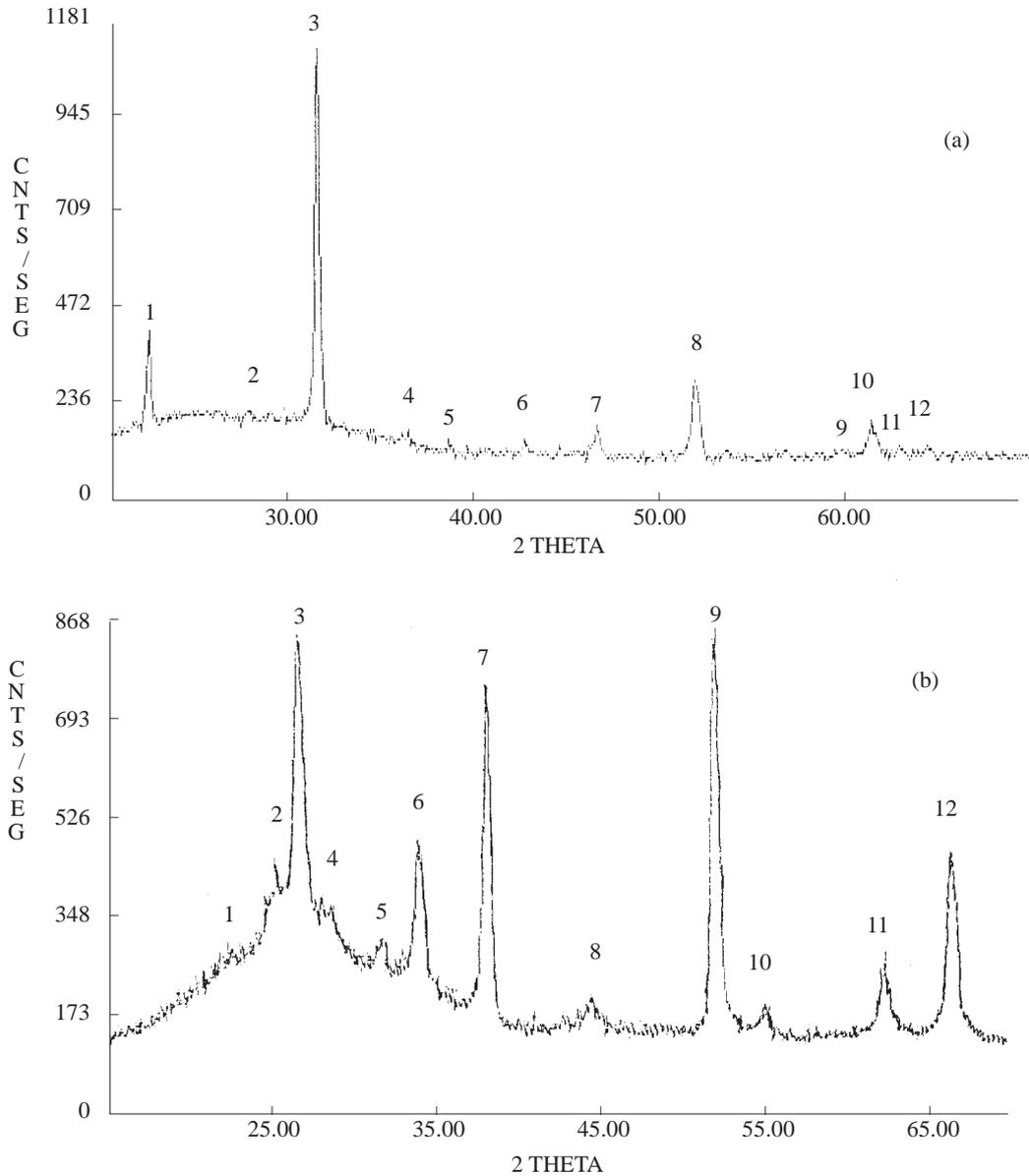
Figure 7. X Ray diffraction of CdS films prepared in 0.2M Cd^{2+}, 0.05 M $S_2O_2^{2-}$, solution at 90°C and pH 3 using HCI in the electrolyte
a) ITO/glass substrate b) Electrodeposited CdS coated ITO/glass

Table 2. Lattice spacing of standard hexagonal and cubic CdS and CdS films on the ITO coated glass substrates.

Hex. CdS (Standard)		Cubic CdS (Standard)		ITO (from substrate)		CdS film (from substrate)	
d (A°)	hkl	d (A°)	hkl	d (A°)	peak no	d (A°)	peak no
				4.0222	1	4.0548	1
3.583	100					3.6011	2
3.367	002	3.36	111			3.4049	3
		2.90	200				
				3.2522	2		
3.160	101					3.1731	4
				2.8746	3	2.8734	5
						2.6880*	6
2.450	102			2.4934	4	2.4021	7
2.068	110	2.058	220			2.0652	8
1.791	200	1.753	311	1.7763	8	1.7813	9
1.679	004	1.680	222			1.6910	10
1.520	104			1.5199	10	1.5099	11
		1.453	400	1.4556	12	1.4287*	12

ITO contains ln_2O_3 +ca 5-10% SnO_2 has the lattice spacing at 2.644, 1.439 and 1.415. So, these peaks (6 and 12) may correspond to SnO_2.

Surface properties

The SEM pictures of the CdS films prepared at different conditions show that:

- A large decrease of clusters was observed for lower pH values.

- More homogeneous crystallisation was formed at lower temperatures (80°C). However, deposition times increase.

- When the H_2SO_4 was used to adjust the pH, the clusters were bigger than those prepared by using HCI in the electrolyte.

- At lower pH values, the shape of crystals is different relatively to crystals obtained at higher pH values and the grain size decreases.

The surface composition was determined by Scanning AUGER Spectrometer. Table 3 shows the results obtained for two different films prepared at two different pH values CI atoms comes from the electrolyte used. Best stoichiometric value of Cd:S has been obtained for pH=3.

Table 3. Surface compositions of CdS films prepared at two different pH values:

pH	Cd	S	O	C	Cl
3	40.6	36.2	3.7	13.7	5.5
2.6	44.4	29.7	5.5	11.7	8.4

Cell Performance

The cell performance of the ED CdS films prepared at pH 3 was also investigated. The CdS/SnO_2 structures were $CdCl_2$ and nitrogen heat treated prior to CdTe deposition to improve their optical and structural properties [25]. This involves the application of a thin coating of $CdCl_2$ to the CdS and a subsequent annealing in inert ambient (N_2) for 30-50 min. CdS pre-treatment has been found to lead to higher and more stable V_{oc} and to suppress CdTe/CdS interdiffusion during the final annealing step of CdTe/CdS film [26]. The cell fabrication process is described elsewhere [26] and consists of a $CdCl_2$ application to the CdTe surface, heat treatment open to air at $400°C$ for 20-30 min, contacting with Au. The dependence of cell parameters for a series of CdS thicknesses are shown in Table 4. The CdS thickness was varied from $500 A°$ to $2500 A°$. A CdS thickness of $1250 A°$ yielded in higher efficiency (η). Enhanced short-circuit photocurrent (J_{sc}) is caused by improved quantum efficiency in the spectral range close to the bandgap of CdS. Cells with very thin ($500 A°$) CdS exhibit low efficiency, caused mainly by a low V_{oc}. An increase of CdS thickness to $2500 A°$ lead also to a significant decrease in V_{oc} (open circuit potential), by ~ 135 mV., resulted in high shunt resistance (R_{sh}) and low efficiencies of the cells.
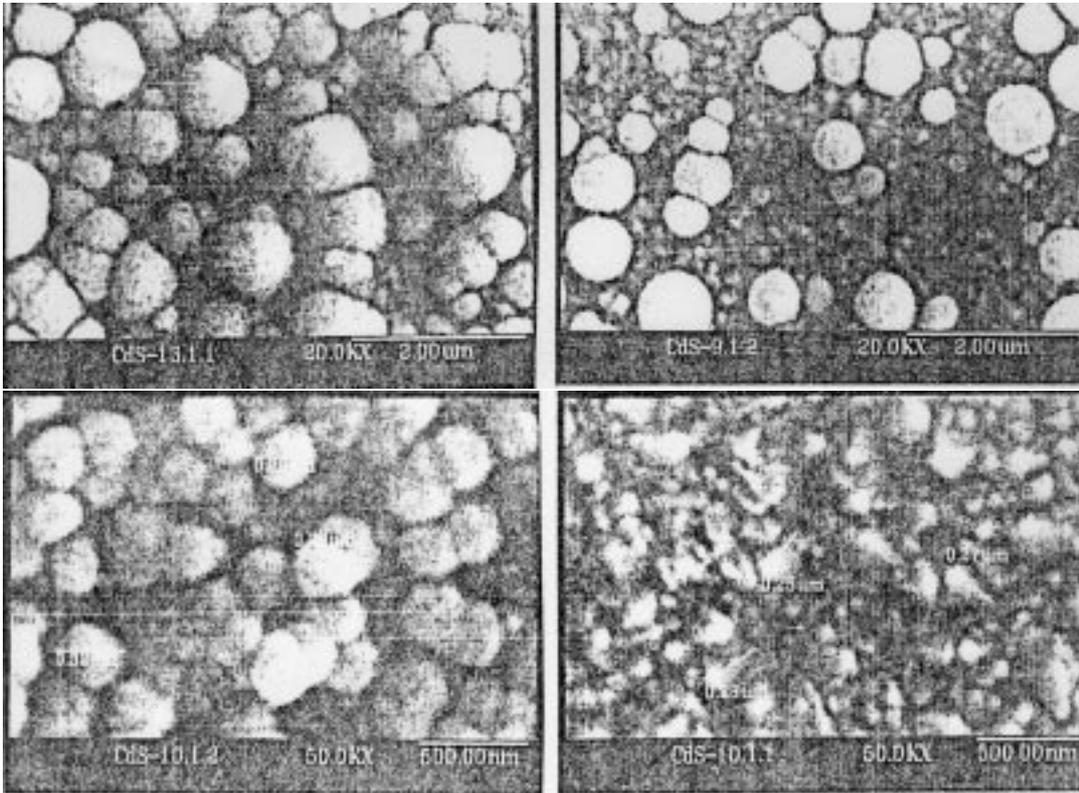
Figure 8. SEM pictures of CdS films prepared in different acids and at different acids and at different pH values ($0.2M\ Cd^{2+}$, $0.05M\ Na_2SO_4$, $90°C$).
a) pH=3, H_2SO_4 b) pH=3, HCl c) pH=2.27, H_2SO_4, d) pH=3, HCl

Table 4. Cell properties

Sample (CdS thickness)	η (%)	V_{oc} (mV)	J_{sc} (mA)	R_{sh} (cm^2)
500 A°	5.73	433	24.5	189
1250 A°	7.68	654	24.4	126
2500 A°	7.30	518	22.6	376

Conclusion

Optimum conditions have been obtained in 0.2M $CdCl_2$ +0.05M $S_2O_3^{2-}$ solution at pH=3 and 90°C.

One of the aims of this work was to compare some properties of CdS films prepared by different methods such as CBD, PVD or sputtering.

Pinhole and particulate fractional areas were very low in the case of ED CdS films. When the samples prepared by electrodeposition and CBD are compared, the crystalline phase of CBD was identified as cubic based, while the electrodeposited one was hexagonal.

During the electrodeposition of CdS films, in the Cd^{2+} concentration range examined, the CdS deposition rate is controlled by the pH. Thiosulfate concentration increases the deposition rate for the pH values higher than 2.5. The effect of temperature is also observed on the deposition time.

The efficacy of using electrodeposited CdS for laboratory scale photovoltaic thin film research was demonstrated by fabrication of CdTe/CdS devices' conversion efficiencies and ED CdS films are found to be promising for he CdS/CdTe cell fabrication.

However, more detailed work with modification processes is needed to increase the efficiency.

Acknowledgements

References

1. F. Kadırgan, Electrochemically Prepared Thin Film Solar Cells in Handbook of Advanced Electronic and Photonic Materials, edited by H. S. Nalwa, Academic Press, New York, in press.

2. K. W. Mitchel, C. Eberspacher, F. Cohen, J. Avery, G. C. Duran and W. Bottenberg, Solar Cells 21, 49 (1988).

3. B. Basol, Solar Cells 23, 69 (1988).

4. P. V. Mayers, Solar Cells, 23, 59 (1988)

5. R. D. Michelson, B. J. Stanbery, J. E. Avery, W. S. Chen, and W. E. Devaney, Proc. 19th IEEE Photovoltaic Specialists Conf. New Orleans LA 1987, p.744

6. K. S. Balakrishnan and A. C. Rastogi, Solar Energy Materials 20, 417 (1990)

7. B. Q, D. Kim, D. L. Williamson and J. U. Trefny, J. Electrochem. Soc. 143, 517 7(1996)

8. A. S. Baranski and W. R. Fawcett, J. Electrochem. Soc. 131,2509 (1984)

9. F. Mondon, J. Electrochem. Soc. 132,319 (1985)

10. E. Fatas, R. Duo, P. Herrasti, F. Arjona and E. Garci-Camarero, 131,2243 (1984)

11. G. P. Power, D. R. Peggs and A. J. Parker, Electrochem. Acta, 26,681 (1981)

12. S. K. Das and G. C. Morris, J. Appl. Phys. 73 (2), 782, (1993)

13. B. E. McCandless, A Mordal, R. W. Birkmire, Solar Energy Mat. and Solar Cells, 36,369 (1995)

14. A. Fischer, C. Narayanswamy, D. C. Grecu, E. Bykov, S. A. Nance, U. N. Jayamaha, G. Contreras-Puente, A. D. Compaan, M. A. Stan, A. R. Mason, Proc. 25th IEEE Photovoltaic Specialists Conf. p.921 (1996)

15. K. Ramanathan, M. A. Contreras, J. R. Tuttle, J. Keane, J. D. Webb, S. Asher, D. Niles, R. Dhere, A. L. Tennant, F. L. Hasoon, R. Noufi, Proc. IEEE 25th Photovoltaic Specialists Conf. p. 837 (1996)

16. B. E. McCandless, R. W. Birkmire, Solar Cells, **31**, 527 (1991)

17. T. L. Chu, S. S. Chu, N. Schultz, C. Wang and C. Q. Wu, J. Electrochem. Soc. 139, 2443 (1982)

18. L. Hernandez, O. Melo, O. Zelaya-Angel and R. Lozada-Morales, J. Electrochem. Soc. 141, 3238 (1994)

19. H. Uda, S. Ikegami and H. Sonomura, J. Appl. Phys. 129, 30 (1990)

20. W. J. Danaker, L. E. Lionc and G. C. Morris, Sol. Energy Mater. 12, 137 (1985)

21. O. de Melo, L. Hernandez, O. Zelaya-Angel, R. Lozada-Morales and M. Becerril, Appl. Phys. Lett. 65, 1278 (1994)

22. I. Kaur, D. K. Pandya, and K. L. Chopra, Solid State Science and Technology, 127, 943 (1980)

23. U. Demir and C. Shannon, Langmuir 10, 2794 (1994)

24. U. Demir and C. Shannon, Langmuir 12, 594 (1996)

25. S. C. Park, B. W. Han, J. H. Ahn, B. T. Ahn and D. Kim, 25th IEEE Photovoltaic Specialists Conf. Washington D. C., 1996

26. W. Song, D. Mao, Y. Zhu, J. Tang and J. U. Trefny, 25th IEEE Photovoltaic Specialists Conf. Washington D. C. 1996